



# Vibrations Induced by Rubbing Between Labyrinth and Rubber-Coating for Rotating Engine in Experiment

Ruixian Ma<sup>1</sup>(✉), Yaqing Wei<sup>1</sup>, Quankun Li<sup>1</sup>, Rui Wang<sup>1</sup>, Mingfu Liao<sup>1</sup>,  
Kaiming Wang<sup>2</sup>, and Pin Lv<sup>3</sup>

<sup>1</sup> Northwestern Polytechnical University, Xi'an 710072, China  
maruixian@nwpu.edu.cn

<sup>2</sup> AECC Commercial Aircraft Engine Co., Ltd, Shanghai 200241, China

<sup>3</sup> Goldwind Science and Technology Co., Ltd, Urumqi 830026, China

**Abstract.** Rotor-stator rubbing is common in rotating engines, and the induced vibrational characteristics of the rotor and stator are affected by the rubbing materials. The soft coating made by vulcanized rubber is considered for rubbing case, followed by the experimental investigations on the kind of progressive rubbing between the seal-labyrinth and the seal-case of a rotor. The vibrational waveforms and the spectral features of the rotor and stator, together with the shaft orbits during the rubbing process are analyzed. The center of the rotor is forced to shift from the balance point of zero displacement, in the meanwhile, the vibrational acceleration of the stator is increased radically and finally nonlinear instability is excited during the rubbing. The shaft orbit varies from stable to unstable, and recovers to be stable eventually. Rotor-stator coupling resonance is captured both in the rotor and stator vibrational signals. High-order super-harmonics (corresponding to the resonance of the rotor and stator), the modulations of the fundamental rotating frequency are excited by the soft rubbing.

**Keywords:** Rotor-Stator Rubbing · Coupling Resonance · Rotating Power Machines

## 1 Introduction

In modern rotating engines, the clearance between the rotor and stator is generally designed to be quite small to reduce the power loss. As a result, the possibility and the severity of rubbing between the rotor and stator is also increased, which may induced by excessive vibration of the rotor. The resulting rubbing generates genitive effects on the engines safety.

In general, two methods can be employed to reduce the effects of rotor-stator rubbing. One is identifying the rubbing characteristics, and then removing the rubbing faults in advance. The other one is attaching abrasible coating on the surface where the rubbing

---

ICANDVC2023 best presentation paper.

occurs to relieve its impacts. Many researchers have contributed to the analysis of rotor vibration under the action of rubbing. Chu et al. [1] and Ma et al. [2] analyzed the vibration of a rotor with rubbing at various rotating speeds. Different features in terms of the sub-harmonics, high-order harmonics and the vibration amplitudes were observed for the rubbing occurring before and after the rotor critical speed. Sun et al. [3] carried out steady-state response analysis for a dual-rotor system rubbing. Additionally, prevent studies show the vibration features of rotor-stator rubbing are affected by the abrasible coating. The results obtained by Batailly et al. [4] suggested that the casing vibration acceleration during rubbing was effectively reduced by the seal coating. Yang et al. [5] simulated the fixed-point rubbing phenomenon with different bump materials on the casing, and the results suggested that softer bump material generated less impacts on the rotor vibration. The thermal effects and the wear of abrasible coating for the blade-casing rubbing were considered in Refs. [6–8]. Their results showed that the blade vibration might strongly depends on the contacting status. Stringer et al. [9] studied the effects of immersing velocity on the wear mechanisms. In the calculations of rubbing between blade and coated casing performed by Berthoulet et al. [10], the results proved the wear appearance along the circumferential direction and radial direction is related to the blade modes. In addition, the wear severity of the coating is strongly relevant to the coating material parameters. In general, published investigations of the rotor-stator coupling vibration for rubbing mainly focused on the type of blade-casing rubbing (especially for the blade resonance). On the other hand, the coatings were basically made of metal-based abrasible material.

In special novel seal structures, rubber has been utilized for the abrasible coating of the casing, in conjunction with labyrinth-teeth manufactured on thin-shell drum-like rotor. This combination of rotor structure and the coating material is significantly different from the traditional design, may resulting in completely vibration features when rotor and stator rub. However, to the authors acknowledgement, relevant studies are rare.

In sight of the limitation mentioned above, an experimental rig is designed for the rotor-stator rubbing test with drum-like rotor and rubber-coated stator in this study. The vibration displacement of the rotor and the acceleration of the stator are measured during the rubbing process, and the vibration signals are analyzed to identify the rubbing induced features.

## 2 Experimental Design

The schematic diagram of the test rig and the locations of vibration sensors are depicted in Fig. 1. The system is mainly consisted of rotor, stator and driven motor. The rotor is supported by three rolling bearings, two of which are located at the free end and the other is at the driven end. In special, the squeeze film damper (SFD) and elastic support are installed for the No.1 bearing at the free end and No.5 bearing at the driven end. As for the rubbing components, the rotor is a kind of thin-shell drum, wherein two labyrinth teethes are manufactured along the circumferential direction as is shown in the enlarged part in Fig. 1. The rubbing stator is a rubber-coated casing. The maximum power of the driven motor is 220 kW, and the maximum speed is 20000 r/min.

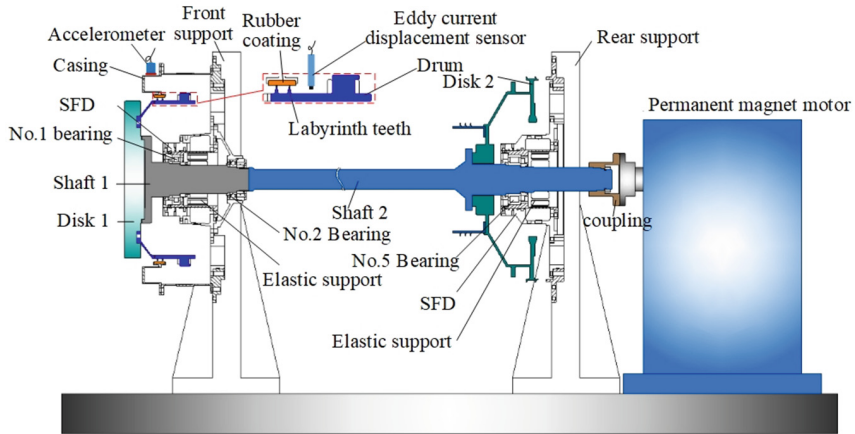


**Fig. 1.** Schematic diagram of test rig.

As can be seen in Fig. 1, the eddy current displacement sensor is adopted to measure the rotor drum vibration both along the horizontal direction and vertical direction. Accelerometer is used to collect the stator casing vibration, which is also installed both along the two directions. The parameters of these two kinds of vibrational sensors are presented in Table 1.

**Table 1.** Parameters of sensors.

Type	Sensitivity	Measurement range	Frequency Range	Location
Eddy current sensor	8 mV/ $\mu\text{m}$	1.5 mm	0–2600 Hz	Rotor (drum)
Accelerometer	100 mV/g	$\pm 50$ g	0–10000 Hz	Stator (casing)

### 3 Results and Discussion

#### 3.1 Results of Rotor Vibration

The variation of rotating speed along with data collecting time is shown in Fig. 2, wherein the speed is increased gradually in stepped form. However, the speed can be noticed to change abruptly around from 426 s to 432 s (as is presented in the enlarged figure of Fig. 2), which indicates the drum and the casing is rubbing. The fluctuation of the rotating speed is induced by the driven torque of the motor and opposing torque generated by rubbing. The rubbing is so serious that the opposing torque overcomes the driven torque, resulting into the deceleration of rotating speed. With the rubbing coating being worn off rapidly, the rotating speed is forced to increase again by the motor driven torque until it reaching the target speed of 2400 r/min.

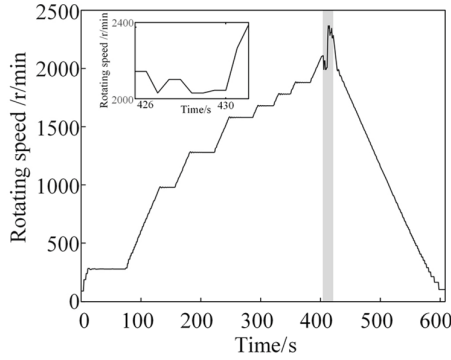


**Fig. 2.** Rotating speed versus time.

The time waveforms of drum displacement during rubbing period are presented in Fig. 3(a) and Fig. 3(b) for the horizontal direction and vertical direction respectively. It can be seen that during the period of 427 s to 429 s (428 s particularly), the displacement waveform in the vertical direction is changed dramatically. This period corresponds to the fluctuation cycle of rotating speed which is observed when sever rubbing occurs. Due to the rotor-stator rubbing, the vibration amplitude is decreased to some extent together with the symmetry breaking around the zero point of the rotor displacement. Conversely, the vibration displacement of drum is recovered to be stale again after 429 s, which indicates the rubbing becoming reduced.

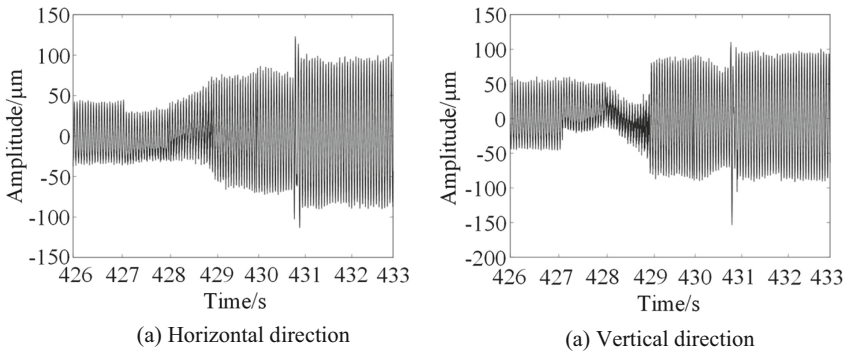


**Fig. 3.** Time waveforms of drum displacement during rubbing.

Figures 4(a)–4(f) demonstrate the rotor orbit of the drum during the rubbing cycle at different rotating speeds with time advancing. As is seen, the rotor orbit is stable at 2121 r/min before rubbing, showing a typical elliptical pattern. When rotor and stator start to rub, the rotor orbit is forced to be unstable relatively with a decrease of rotating speed to 2098 r/min. As the rubbing being more serious, the rotor orbit shows a chaos status, in agreement with the displacement waveforms at 428 s with a speed of 2031 r/min. After the rapid wear of rubber coating of the casing by the labyrinth teeth, the clearance between

the coating and labyrinth teeth is increased gradually, contributing to the recovery of rotor orbit stability, as illustrated from Figs. 4(d) to Figs. 4(f).

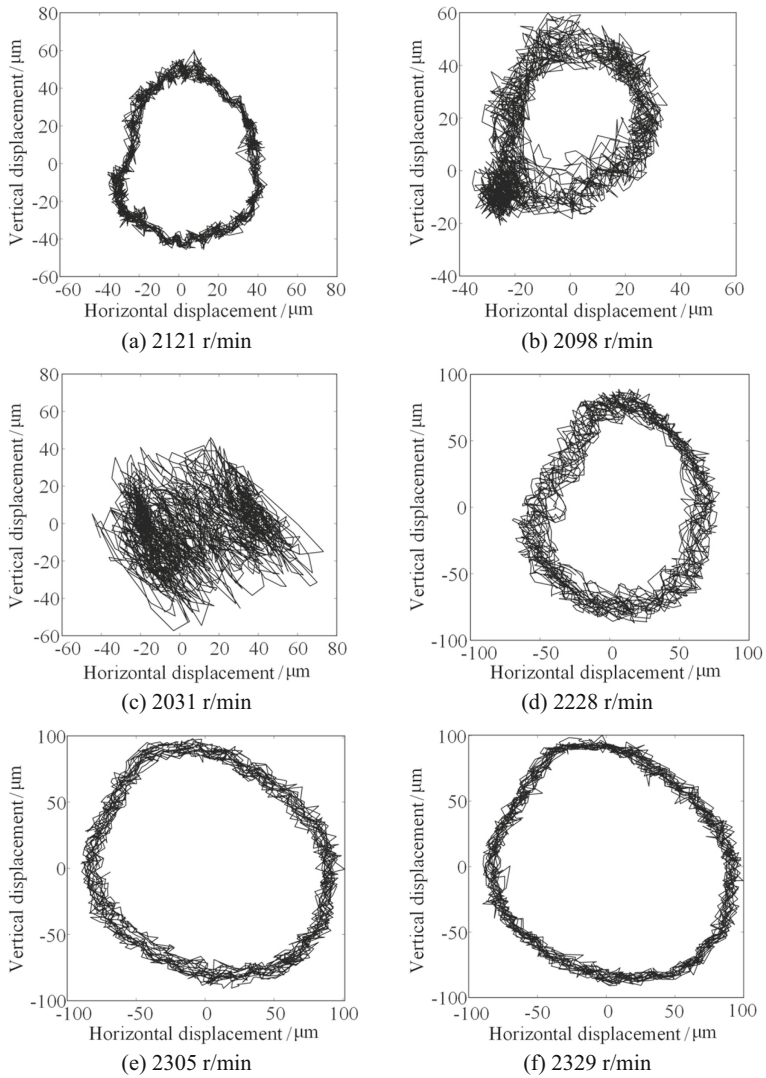


**Fig. 4.** Rotor orbit of the drum during rubbing.

For comparison, the rotor orbits of the drum without rubbing at corresponding typical speed of Fig. 4 are depicted in Fig. 5, wherein stable vibration of the drum can be observed at all speeds distinctly. The comparisons with respect to Fig. 4 further suggest that the serious unsteady movements of the rotor at Figs. 4(b) and Figs. 4(c) are excited by the rotor-stator rubbing.

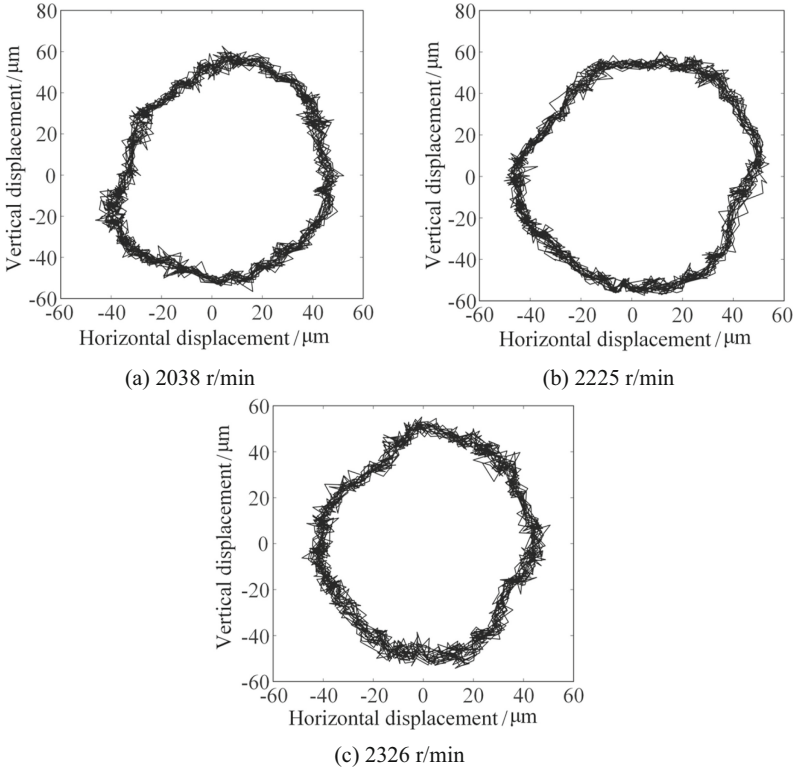


**Fig. 5.** Rotor orbit of the drum without rubbing.

For the purpose of investigating the spectral features of rubbing induced vibration, Figs. 6(a)–Figs. 6(f) show the spectrums of drum displacement during rubbing in consistent with the rotating speeds in Fig. 4. As can be seen in Fig. 6(a), at the initial stage of rubbing the effects of rotor-stator contacting and friction are completely small that the dominated frequencies are the fundamental rotating frequency 35.38 Hz as well as the 2X component. With rubbing being serious (Figs. 6(b) and 6(c)), several higher order harmonics vibration are excited, including the 6X and 8X components. As for the vibration at 482.8 Hz in Fig. 6(c) (as well as 490 Hz in Figs. 6(d)–6(e)) and at 750 Hz in Figs. 6(b)–6(c), these components are contributed to the rotor-stator coupling vibration. In particular, the vibration at 750 Hz corresponds to the natural frequency of the casing, which will be shown in Sect. 3.2. The component around 490 Hz is attributed to the first order resonance of the drum as can be seen in Fig. 7. From Figs. 6(d)–6(f), the vibration

frequency of the drum gradually changed to be dominated by the fundamental frequency again, indicating the negligible effect of rubbing.

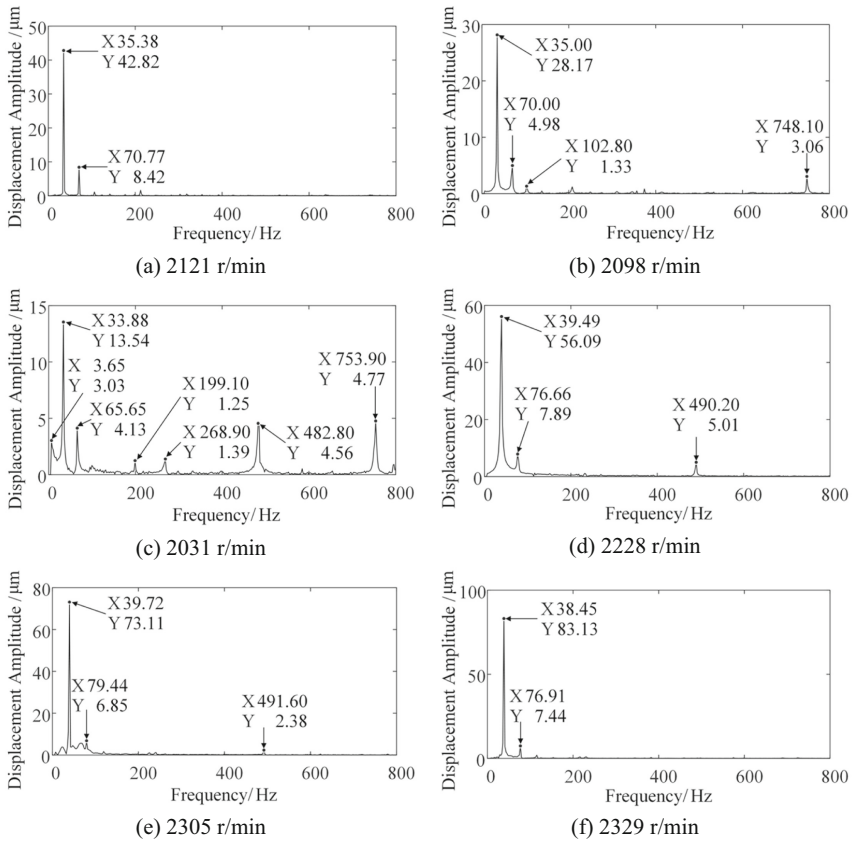


Fig. 6. Spectrums for drum displacement during rubbing.

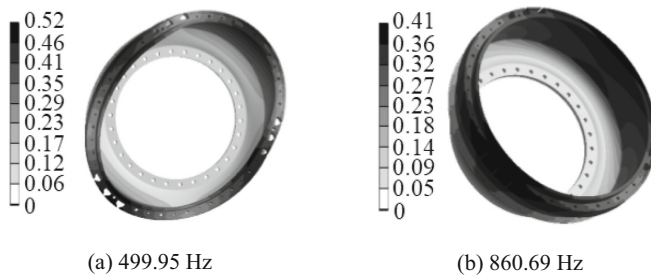
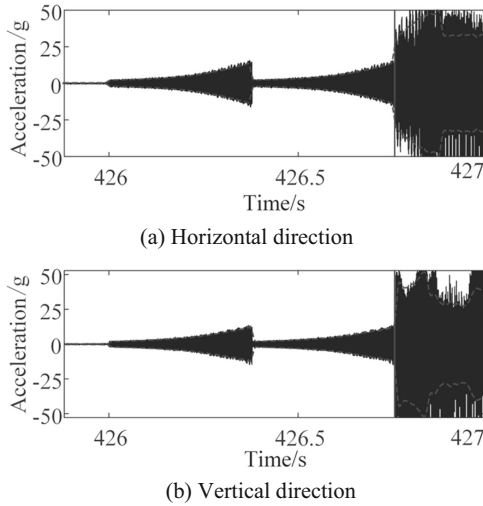


Fig. 7. Natural frequencies and modes of rotor drum.

### 3.2 Results of Stator Vibration

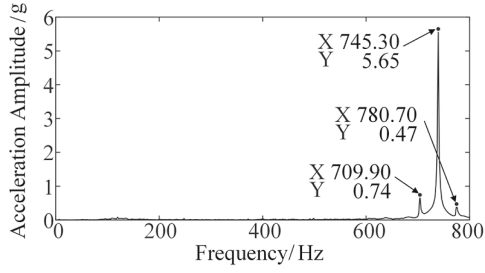
The time waveforms of vibration acceleration of casing during rubbing period are presented in Fig. 8, wherein the horizontal and vertical vibrations are shown in Fig. 8(a) and 8(b) respectively. It can be seen that the initial phase of rubbing between 426s and 426.5 s, the vibration acceleration of casing increases gradually, nevertheless a sharp drop of acceleration amplitude can be noticed. After the sharp drop, the vibration amplitude shows a repetitive increase as before. However, at about 426.8 s, the acceleration amplitude abruptly increases to over 50 g, indicating the nonlinear instability phases of the casing under the action of rubbing.



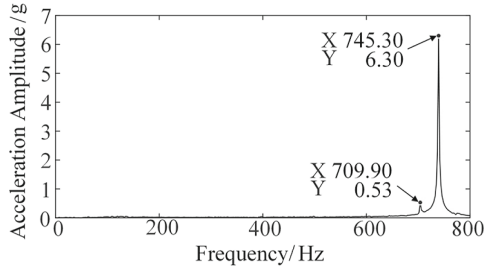
**Fig. 8.** Time waveforms of acceleration for rubbing casing.

Figure 9 presents the Fourier transform results for the data of the first gradually-increase phase in Fig. 8, and the corresponding rotating speed is 2123 r/min. The characteristic frequency around 745 Hz can be noticed easily. This frequency is in agreement with the frequency of 750 Hz observed in rotor vibration. On the contrary, the vibration at the rotating frequency is negligible. In order to confirm the vibration source of the dominant frequency 745 Hz, the calculated first four orders of natural frequency and modes of casing are shown in Fig. 10. The fourth order frequency of 774 Hz can be noticed, which is identically in coincident with the characteristic frequency captured both for rotor and stator at around 750 Hz. Therefore, the rubbing excited resonance of the casing may contribute significantly to both rotor and stator vibration. In addition, modulated side-band can be observed at 709.9 Hz and 780.7 Hz, which are modulated by the resonance frequency 745 Hz of the stator and the rotating frequency of the rotor.





(a) Horizontal direction



(b) Vertical direction

**Fig.9.** Spectrums of acceleration for rubbing casing.

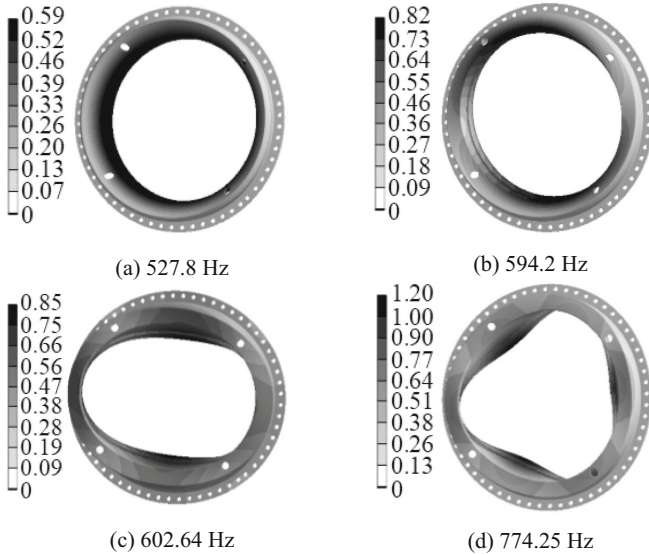


**Fig. 10.** Natural frequencies and modes of casing.

## 4 Conclusions

Vibration induced by the rubbing between a seal-labyrinth of drum-like rotor and a rubber-coated casing is investigated experimentally and the results are discussed both for the rotor displacement and stator acceleration. When the rubbing is serious, the center of the rotor is forced to shift from the balance point of zero displacement, along with the decrease of rotating speed. Both the higher order harmonics of 6X and 8X and the natural frequencies of the drum and the casing are excited by the rubbing. Strong coupling between the rotor and stator vibration can be identified. The natural frequencies of the drum and the casing all can be captured in the spectrums of the rotor vibration displacement. The vibration of the casing shows a character of nonlinear instability under the action of serious rubbing. A modulation between the rotating frequency and the stator natural frequency arises.

**Acknowledgements.** The financial support from the National Key Research and Development Program (Grant 2022YFB4201400), the Innovation Capability Support Program of Shaanxi (Grant 2023-CX-TD-30), China Scholarship Council (202306290109) and the Fundamental Research Funds for the Central Universities (Grant D5000210481, 31020200QD705) is gratefully acknowledged.

## References

1. Chu, F.L., Lu, W.: Experimental observation of nonlinear vibrations in a rub-impact rotor system. *J. Sound Vib.* **283**(3–5), 621–643 (2005)
2. Ma, H., Shi, C., Han, Q., et al.: Fixed-point rubbing fault characteristic analysis of a rotor system based on con-tact theory. *Mech. Syst. Sig. Process.* **38**, 137–153 (2013)
3. Sun, C., Chen, Y., Hou, L.: Steady-state response characteristics of a dual-rotor system induced by rub-impact. *Nonlinear Dyn.* **86**, 91–105 (2016)
4. Batailly, A., Legrand, M.: Unilateral contact induced blade/casing vibratory interactions in impellers: analysis for flexible casings with friction and abradable coating. *J. Sound Vib.* **348**, 344–364 (2015)
5. Yang, Y., Cao, D.Q., Xu, Y.Q.: Rubbing analysis of a nonlinear rotor system with surface coatings. *Int. J. Non-Linear Mech.* **84**, 105–115 (2016)
6. Millecamps, A., Brunel, J.F., Dufrenoy, P., et al.: Influence of thermal effects during blade-casing con-tact experiments. In: *Proceedings of the ASME 2009 International Design Engineering Technical Conferences and Computers and Information in Engineering Conference*, DETC2009-86842, San Diego (2009)
7. Nyssen, F., Batailly, A.: Sensitivity analysis of rotor/stator interactions accounting for wear and thermal effects within low-and high-pressure compressor stages. *Coatings* **10**(1), 74.1–74.23 (2020)
8. Agrapart, Q., Nyssen, F., Lavazec, D., et al.: Multi-physics numerical simulation of an experimentally predicted rubbing event in aircraft engines. *J. Sound Vib.* **460**, 114869.1–114869.25 (2019)
9. Stringer, J., Marshall, M.B.: High speed wear testing of an abradable coating. *Wear* **294–295**, 257–263 (2012)
10. Berthoull, B., Batailly, A., Stainier, et al.: Phenomenological modeling of abradable wear in turbomachines. *Mech. Syst. Sig. Process.* **98**, 770–785 (2018)